Acta Geophysica
https://doi.org/10.1007/s11600-019-00379-y

RESEARCH ARTICLE - HYDROLOGY

The added value of spatially distributed meteorological data for simulating hydrological processes in a small Mediterranean catchment

Ahlem Gara[1,2] · Khouloud Gader[2] · Slaheddine Khlifi[1] · Marnik Vanclooster[3] · Donia Jendoubi[4] · Christophe Bouvier[5]

Received: 14 August 2018 / Accepted: 17 October 2019

Abstract
The purpose of this paper was to demonstrate the added value of the spatial distribution of rainfall and potential evapotranspiration (PE) in the prediction of the discharge for a small Mediterranean catchment located in the Medjerda basin in Tunisia, i.e. the Raghay. We compare therefore the performance of a conceptual hydrological model available in the ATHYS platform, using global and spatial distributed input data. The model was implemented in two different ways. The first implementation was in a spatially distributed mode, and the second one was in a non-distributed lumped mode by using spatially averaged data weighed with a Thiessen-interpolated factor. The performance of the model was analysed for the distributed mode and for the lumped mode with a cross-validation test and through several modelling evaluation criteria. Simultaneously, the impact of the spatial distribution of meteorological data was assessed for the two cases when estimating the model parameters, the flow and water amounts, and the flow duration curves. The cross-validation of the split-sample test shows a preference for the spatially distributed model based on accuracy criteria and graphical comparison. The distributed mode required, however, more simulation time. Finally, the results reported for the Raghay indicated that the added value of the spatial distribution of rainfall and PE is not constant for the whole series of data, depending on the spatial and temporal variability of climate data over the catchment that should be assessed prior to the modelling implementations.

Keywords Medjerda · ATHYS · Hydrological modelling · Distributed PE and rainfall · Accuracy criteria

Introduction

The assessment of the water resources as support for water management can be based either on monitoring or hydrological modelling programs (Ibrahim et al. 2015). In Africa, however, the hydrological monitoring programs are often deficient. Hydrological monitoring gauges are often limited to a few observed stations, mainly focused on the main watersheds within a region. Small watersheds of less than one thousand square kilometres are generally not well monitored (Schuol et al. 2008; Ibrahim et al. 2015). For small water catchments with limited data, hydrological modelling remains the second option to assess the water resources and different hydrological functions (Oudin et al. 2008; Coustau et al. 2012; Tegegne et al. 2017). Rainfall–runoff (RR) models are therefore essential tools that support decision-making and water management (Andréassian et al. 2004).

Distributed hydrological RR models are now very popular because they can describe rainfall–runoff response

✉ Ahlem Gara
ahlem_gara@yahoo.fr

1 U-R:Gestion Durable des Ressources en Eau et en Sol (GDRES), High School of Engineering of Medjez el Bab (ESIM), University of Jendouba, Jendouba, Tunisia

2 National Agronomic Institute of Tunisia (INAT), University of Carthage, Tunis, Tunisia

3 Earth and Life Institute, Université Catholique de Louvain, Louvain-la-Neuve, Belgium

4 Centre for Development and Environment (CDE), University of Bern, Bern, Switzerland

5 HydroSciences Montpellier, Institut de Recherche pour le Développement (IRD), Montpellier, France

Published online: 25 October 2019

with spatially distributed input, which can be managed with modern GIS and remote sensing technology (Bao et al. 2017). A more detailed representation of the spatial variability in RR modelling is definitely sounder from a conceptual basis. Distributed RR modelling is, however, subjected to a lot of uncertainties. The uncertain representation of the hydrological modelling input is an example. Uncertainties related to the spatial variability of climate data have been demonstrated to affect hydrological modelling performance (Sangati and Borga 2009). Distributed RR modelling may also become constraining from an operational perspective. When implementing an RR model, an appropriate selection has to be made considering the trade-offs between model efficiency, validity and robustness (Duan et al. 2003). Model identifiability, i.e. the capacity to implement and parameterize the model in an operational context, can be considered as a part of model efficiency (Gábor et al. 2017). Model identifiability will be high when the model structure is simple; it will be low when the model structure is complex. Hence, spatially distributed hydrological models may suffer from identifiability issues.

In order to reduce the complexity and hence increase the identifiability of distributed RR models, it will be interesting to reduce the number of parameters. A straightforward strategy consists in running the spatially distributed model with partially lumping a part of the spatially distributed parameters. Although it is assumed that such lumping will generally reduce model performance in terms of goodness of fit, the associated results may remain acceptable in terms of identifiability. It is therefore important to analyse carefully the trade-off between goodness of fit and overall modelling efficiency. This problem has been largely studied, and many viable results have been found when focusing on comparing between lumped and distributed modes' performance in order to pick out the best-selected model based on its performance and the running duration. Brulebois et al. (2018) confirmed that the results given by two models, a semi-distributed physically based model SWAT and a global conceptual model GR4j, are rather close when tested over contrasted climate periods, with slightly higher robustness for the SWAT model. In the same context, Coustau et al. (2012) brought to the light the important benefits for the use of distributed hydrological models that take into account the radar data without increasing the number of parameters or the complexity of the model. However, distributed models do not always give better results than the lumped models. Vansteenkiste et al. (2014) found out that lumped models actually gave similar results as the distributed models based on accuracy criteria for different spatial resolutions. Both types of models produced well the seasonality with a preference to lumped models, especially for overall water balance terms and subsurface flow.

Similarly, Khakbaz et al. (2012) certified that lumped implementations were able to sufficiently endorse the effects of spatial variability in precipitation on stream-flow prediction. These results were consistent with those found in many studies comparing lumped and distributed hydrological models, suggesting that the two types of model scan give similar results in terms of accuracy and that there is no superior model if several measures of model performance are considered (Ajami et al. 2004; Breuer et al. 2009; Koren et al. 2012; Apip et al. 2012; Lobligeois et al. 2014). According to Lobligeois et al. (2014), the results are largely determined by the catchment complexity and the existing spatial and temporal variability of the hydro-climatic data. Yet, the way how catchment complexity and spatial and temporal variability of hydrologic attributes determines the ultimate performance of distributed versus lumped models needs further investigation.

This paper aims to contribute to this challenge by addressing the following question: How can spatially distributed climate data improve hydrological model prediction in poorly gauged catchments? We select to address this issue of the Raghay catchment which is a small sub-catchment of the Medjerda basin in Tunisia. The Medjerda is suffering from hydrometric data availability in quantity and in quality, which jeopardizes the management of droughts and floods that typically characterize the Mediterranean regions (Ludwig et al. 2011). While analysing this aspect, we also try to answer the following scientific question: Is the selected hydrological conceptual model suitable for reproducing the hydrological response in the Raghay catchment?

In an attempt to respond to this question, the paper is organized as follows: In the first part, a concise description of the runoff and the routing models that are used is given. In addition, the adopted validation method is summarized. The second section describes the study site, followed by a presentation of the available data used to run the model. The third part of this paper illustrates and discusses the use of reanalysis hydro-climatic data in addition to the observed ones. This is followed by an outlining of the main results for the two calibration phases by comparing the goodness of fit, scatter plots and flow duration curves when implementing a conceptual runoff hydrological model in a fully spatial distributed mode (case 1) and in a lumped mode (case 2). The final section summarizes the main conclusions of the paper.

Rainfall–runoff modelling implementation

We implemented RR models for the catchment using the hydrological modelling platform ATHYS (Atelier Hydrologique Spatialisé, Bouvier et al. 2013). This open and free-use software platform (www.athys-soft.org) is continuously updated to allow the improvement of results and

to minimize the simulation time. It presents the possibility to combine many production functions and transfer functions via a consistent and easy-to-use environment, including processing of hydro-meteorological and geographical data. For our case study, we decided to use a modified distributed version of the runoff model of the Soil Conservation Service (SCS) with the integration of potential evaporation (PE) combined with a lag-and-route (LR) routing model. The SCS model was widely used to predict runoff, especially for poorly gauged catchments (Mishra et al. 2003). The LR routing model was also tested in several catchments in southern France (Bentura and Michel 1997; Tramblay et al. 2011).

The model was implemented in two different ways: once in a fully spatial distributed mode (case 1), by using distributed rainfall and PE input data, and once in a non-distributed lumped mode (case 2), by using averaged rainfall and PE input weighted by Thiessen coefficients (Table 1).

This distributed model operates over a grid mesh of regular cells using as input the digital elevation model and permitting the generation of its derived maps such as slopes, flow directions and sub-basin layers (Gara et al. 2015). The time step used to run the model is a daily time step for continuous hydro-climate data to permit taking into account the dry and the wet phases of the hydrological cycle and based on the available data series for a long enough period of observations. Rainfall and PE were interpolated using Thiessen interpolation method and were integrated into the runoff model in order to calculate flows for each grid cell. The LR model processed the elementary hydrograph for each cell and routed this hydrograph to the discharge point of the catchment to provide a complete simulated runoff (Bouvier et al. 2008).

The modified runoff model with PE integration

The Soil Conservation Service (SCS) model, developed by US Soil Conservation Service, has been largely used for estimating runoff from medium- and small-sized watersheds (Hawkins 1993; Lewis et al. 2000; Liu and Li 2008; Tramblay et al. 2011). The model was also applied to model runoff in Tunisian catchments (Sellami et al. 2013; Dakhlaoui et al. 2017) based on the fact that this model requires only commonly available terrain data. In this paper, we associated the Soil Moisture Accounting (SMA) procedure to the SCS method in the ATHYS platform.

We used here the SCS–SMA formulated by Michel et al. (2005), relating rainfall and runoff based on the relationship between:

$$\begin{aligned} R(t) &= p(t) \times \left(\tfrac{V(t)-\mathrm{Sa}}{S}\right) \times \left(2 - \tfrac{V(t)-\mathrm{Sa}}{S}\right) \quad \text{if } \mathrm{V}(t) > \mathrm{Sa} \\ R(t) &= 0 \quad \text{otherwise} \end{aligned} \tag{1}$$

where $R(t)$ [L T^{-1}] denotes the runoff rate, $p(t)$ [L T^{-1}] the rainfall intensity at the time t, S[L] the maximal capacity of the soil reservoir, $V(t)$ the level in the soil reservoir at the time t[L] and Sa[L] the initial losses.

The advantage of this model is that the runoff is directly related to the level in the soil reservoir, which eases the use of discharge of this soil reservoir and the formulation of a delayed runoff as a part of this discharge (Fig. 1).

The runoff rate, $R(t)$, can be simplified as the product of the runoff coefficient $C(t)$[−] and rainfall intensity at time t, $p(t)$, where

$$C(t) = \left(\frac{V(t) - \mathrm{Sa}}{S}\right) \times \left(2 - \frac{V(t) - \mathrm{Sa}}{S}\right) \tag{2}$$

The soil reservoir is then forced by the intensity of infiltration at time t, $f(t)$ [L T^{-1}], which is expressed as follows:

$$f(t) = (1 - C(t)) \times p(t) \tag{3}$$

To consider the reduction in the runoff coefficient for non-rainy periods, we used the linear emptying intensity coefficient of the soil reservoir at time t, $E(t)$ [L T^{-1}], to

Table 1 Summary description of the methodology used for the two cases of modelling in the Raghay catchment

	Case 1	Case 2
Model description	Distributed SCS–SMA–ETP–simple lag-and-route model	Lumped SCS–SMA–ETP–simple lag-and-route model
Model parameters	S, ω, Sa/S, ds, V_0, K_0	S, ω, ds, Sa/s, V_0, K_1
Input description	*Spatially distributed observed rainfalls (data from six rainfall stations, 18-year duration) *Spatially distributed PE (data from five climatic CFSR data + 1 climatic observed station, 18-year duration) *DEM[a] (30 m × 30 m)	* Averaged observed rainfalls (Thiessen interpolated from six rainfall stations, 18-year duration) *Averaged PE (Thiessen interpolated from five climatic CFSR data + 1 climatic observed station, 18-year duration) *The watershed is considered as one cell
Output description	Simulated runoff as the sum of all the EH produced for each cell	Simulated runoff in only one EH
Cross-validation accuracy criteria	NS, RMSE, RSR, PBIAS, EFF	

[a]Digital Elevation Model obtained from the mission of 19 June 2014: https://gdex.cr.usgs.gov/gdex/

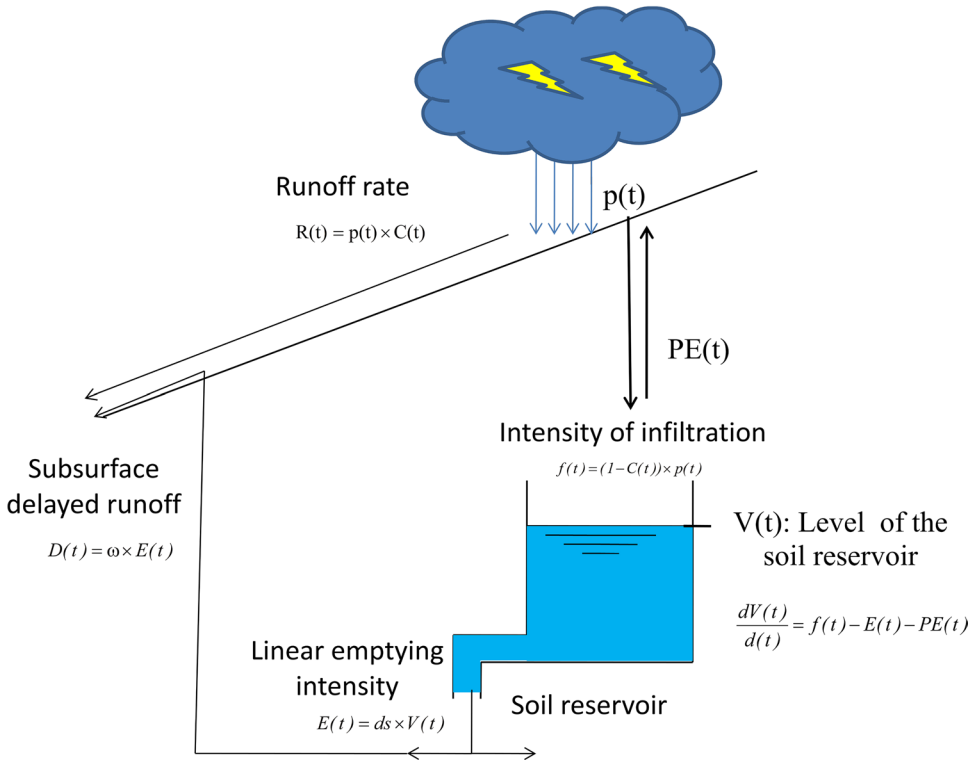

Fig. 1 Simplified presentation of the runoff model

be dependent on the level $V(t)$ in the soil reservoir and the discharge coefficient ds [T^{-1}]:

$$E(t) = \mathrm{ds} \times V(t) \tag{4}$$

assuming to simplify the discharge coefficient due to losses by percolation to the deep aquifer and lateral flow, ds, into a constant parameter over the catchment permitting the decrease in the runoff coefficient during non-rainy periods. Theoretically, we can subdivide the parameter ds into two parts: ds1 taking account of the losses by delayed flow caused by the lateral flow and ds2 which is considering the part of percolation to the deep aquifer.

A part ω of this discharge flows back to the outlet of the catchment, as subsurface-delayed runoff (Coustau et al. 2012).

This additional runoff $D(t)$ [L T^{-1}]:

$$D(t) = \omega \times E(t) \tag{5}$$

must be added to the surface runoff. In the model, a simple presentation of the hydrological process led to neglecting the part of the delayed runoff caused by the percolation to the deep aquifer. Then, ds2 is set into 0 and ds1, which is directly related to the subsurface-delayed runoff, which can be replaced by ω in the calibrated parameters.

The total calculated runoff $R_t(t)$ [L T^{-1}] given by the SCS–SMA procedure is then expressed as follows:

$$R_t(t) = p(t) - f(t) + D(t) \tag{6}$$

The reservoir level $V(t)$ is derived from the balance between the water input (infiltration) and the water output (PE, reservoir discharge due to deep percolation and subsurface flow):

$$\frac{\mathrm{d}V(t)}{\mathrm{d}(t)} = f(t) - E(t) - \mathrm{PE}(t) \tag{7}$$

where the initial level of the soil reservoir is V_o[L].

Definitely, the SCS–SMA model in this simplified version compromises five parameters to be calibrated: the maximal capacity of soil reservoir S [L T^{-1}], the coefficient of the linear emptying of the soil reservoir only by percolation to the deep aquifer ds2 [T^{-1}], the part of the soil discharge to simulate the delayed runoff ω (dimensionless), the fraction limiting the lateral emptying of the reservoirs Sa/S (dimensionless), and the initial level in the soil reservoir V_o [L].

The used formula to calculate the PE is developed by Oudin et al. (2005).

$$\begin{aligned} \mathrm{PE} &= \frac{\mathrm{Re}}{\lambda} \times \frac{\mathrm{Ta}+5}{100} && \text{if } \mathrm{Ta} + 5 > 0 \\ \mathrm{PE} &= 0 && \text{otherwise,} \end{aligned} \tag{8}$$

where PE (mm/day), Re is extraterrestrial radiation (MJ/m^2 day), λ is the latent heat flux (MJ/kg) and Ta is the mean daily air temperature (°C), derived from the long-term average.

The used formula to calculate the PE relies on the results obtained by Andréassian et al. (2004) and Oudin et al. (2005)

when comparing results for the 27 PE-tested formulations. These results proved that a very simple version method which only requires extraterrestrial radiation and mean daily temperature is a sufficient and robust method compared to more complex methods.

Routing model

The SCS–SMA model was connected to the LR routing model. This LR model allows the runoff to be routed from every grid cell to the discharge point of the catchment (Coustau et al. 2012) (Fig. 2). The calculation of the time of travel, T_m, is given by:

$$T_m = \sum \frac{l_k}{V_k} \tag{9}$$

where l_k and V_k are, respectively, the lengths and the velocity over the k-cells of the trajectory between the cell m and the outlet. Here, V_k will be assumed to be uniform and constant at the catchment scale, $V_k = V_o$, for the sake of simplicity.

For each grid cell, the time of propagation (T_m) was forecasted by the routing model and a diffuse time (K_m) is computed as follows:

$$K_m = K_0 \times T_m \tag{10}$$

where K_o (dimensionless) is the diffusion coefficient (lag), which has been preset to 0.7.

The elementary discharge $q(t)$ due to the runoff $R(t_0)$ of cell m at time t_0 (Tramblay et al. 2011) is calculated as follows:

$$\begin{aligned} q_m(t) &= 0 && \text{when } t < t_0 + T_m \\ q_m(t) &= \frac{R(t_0)}{K_m} \exp\left(-\frac{t-(t_0+T_m)}{K_m}\right) \cdot A && \text{otherwise} \end{aligned} \tag{11}$$

Then, the final obtained runoff for the catchment consists of the sum of all the elementary hydrographs produced at the outlet of each grid cell.

When the LR model is used in the lumped case, only one cell is considered, of which the area equals the total area of the catchment. Therefore, there is only one elementary hydrograph produced at the outlet. It yields the simulated runoff, routed to the outlet by means of a simple linear reservoir, with one parameter K_1 (mn), to be calibrated. The V_o parameter is no more useful and should be set to a high value ($V_0 = 1000$ m/s).

The parameters of the LR model to be calibrated are thus either V_0 in distributed mode (K_0 is empirically set to 0.7) or K_1 in lumped mode. The production parameters are the same than those for the distributed model and are considered to be constant over the Raghay catchment; then, the distribution only concerned the rainfall and PE interpolated for each cell.

Cross-validation procedure and performance evaluation

The model performance was assessed for the two cases: (1) distributed mode and (2) lumped mode, using a split-sample cross-validation test (Klemeš 1986). Since we have access to a 18 years' time series of hydro-climatic data, we subdivided this series of data into two equal parts. The first part (P1) presents data going from September 1990 to August 1999, and the second part (P2) includes data ranging from September 1999 until August 2008. Afterwards, we went through a calibration for P1 and validation for P2. This operation is called the first step of the split-sample test procedure. Subsequently, we switched the data by using P2 for the calibration and P1 for the validation for the second step of the cross-validation. In order

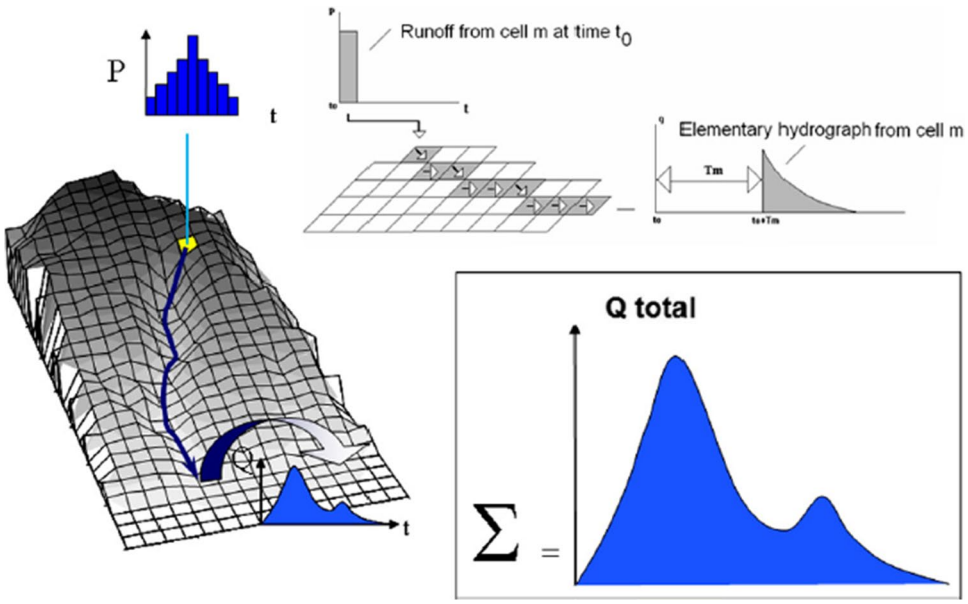

Fig. 2 Diagram of the lag-and-route routing model (Tramblay et al. 2011)

to obtain the parameters for calibration for the two steps of the cross-validation, we used the BLUE (best linear unbiased estimator) algorithm.

The BLUE algorithm, also referred to the error covariance matrix analysis method, is a method of optimization allowing to minimize a cost function (evaluation criteria) based on both the differences between values simulated by the model and observed values (volumes, flow rates, soil moisture content, velocities, etc.), and the differences between initial and optimal values of the model parameters (Henderson 1975). This method is derived from the formulation of the Sherman–Morrison–Woodbury algorithm (Sherman and Morrison 1950). The minimization algorithm of the cost function is based on a gradient method allowing to minimize the running time of the model and then to converge rapidly. The adopted version for the ATHYS platform introduces constraints on the variations of the parameters to be optimized. These constraints are directly linked to the confidence of their initial estimate. This method allows optimizing all the parameters to be calibrated in the RR model. However, the user must specify confidence levels on parameter estimates and observations. The user must also specify the increment (disruption) steps for calculating the derivative of the incremental cost function. Therefore, the number of iterations in the optimization procedure corresponds to an effective realization of an equivalent number of iterations. Then, this optimization is essentially based on the knowledge of the user of the hydrological behaviour for the studied catchment in addition to the status and parameter estimation of the model.

We assessed the runoff prediction accuracy of the model by calculating several performance indicators for hydrological modelling such as the Nash–Sutcliffe efficiency (NS) (Nash and Sutcliffe 1970), the root-mean-square error (RMSE), the ratio of RMSE to the standard deviation of the observations (RSR) (Moriasi et al. 2007) and the Percent BIAS (PBIAS) (Singh et al. 2005). These performance indicators are, respectively, expressed as follows:

$$\mathrm{NS} = 1 - \frac{\sum_{i=1}^{n} \left(S_i - O_i\right)^2}{\sum_{i=1}^{n} \left(O_i - \bar{O}\right)^2} \tag{12}$$

$$\mathrm{RMSE} \sqrt{\frac{\sum_{i=1}^{n} \left(S_i - O_i\right)^2}{N}} \tag{13}$$

$$\mathrm{RSR} = \frac{\left(\sqrt{\sum_{i=1}^{n} \left(O_i - S_i\right)^2}\right)}{\left(\sqrt{\sum_{i=1}^{n} \left(O_i - \bar{O}\right)^2}\right)} \tag{14}$$

$$\mathrm{PBIAS} = \frac{\sum_{i=1}^{n} \left(O_i - S_i\right)}{\sum_{i=1}^{n} \left(O_i\right)} \times 100 \tag{15}$$

where O_i is the observed runoff; S_i: the simulated runoff; $\bar{O}$: the mean observed runoff; n: the number of pairs of the measured and simulated variables.

The NS is widely used for efficiency determination of hydrologic models. It is considerably acceptable when it is greater than 0.5 (Wöhling et al. 2013).

The RMSE is widely used as a goodness-of-fit indicator that describes the difference between the observed and predicted values in the same units. Smaller RMSE values describe a better model for runoff prediction. The RSR can also provide additional information and can be applied to a variety of different constituents. The RSR is considered satisfactory when it is below 0.7.

Similarly, the PBIAS quantifies a model's tendency to underestimate or overestimate values, where a value of zero (optimum) shows a perfect fit. Positive (negative) bias results indicate model underestimation (overestimation). PBIAS is considered satisfactory when it is below 0.25. A performance rating based on PBIAS was used by Moriasi et al. (2007).

To further compare between the simulation of the two model implementations at the same time, we calculated the EFFiciency index (EFF) (Brocca et al. 2010), which is expressed as follows:

$$\mathrm{EFF} = 1 - \frac{\sum \left(Q_{\mathrm{sim\_distributed}}(t) - Q_{\mathrm{Obs}}(t)\right)^2}{\sum \left(Q_{\mathrm{sim\_global}}(t) - Q_{\mathrm{Obs}}(t)\right)^2} \tag{16}$$

where $Q_{\mathrm{sim\_distributed}}$ is the simulated discharge with spatial rainfall and PE.

$Q_{\mathrm{sim\_global}}$ is the simulated discharge using mean Thiessen-interpolated rainfall and PE in the lumped model, and Q_{Obs} is the observed discharge.

The EFF has been used to evaluate the efficiency of spatially distributed meteorological data compared to uniform meteorological data for RR modelling. If EFF is greater than 0, then the use of spatially distributed rainfall produces an improvement in the runoff simulation by the model (Tramblay et al. 2011).

These quantitative evaluations were reinforced by visually evaluating the model performance in comparison with the combined observed and estimated runoff values through scatter plots.

To additionally enhance the emphasis of the spatial variability for the observed rainfalls in the Raghay catchment, we introduced a climatic index calculated for the two parts of the data, P1 and P2. The Standardized Precipitation Index (SPI), developed by Mckee et al. (1993), is mainly used in order to outline and to quantify the shortage or the

abundance of the precipitation in regional or local scale for a specified period. This index remains an effective and flexible tool to highlight the severity of the drought (Zkhiri et al. 2019).

This index is expressed as follows:

$$\mathrm{SPI12} = \frac{P_i - P_{\mathrm{m}}}{\sigma} \tag{17}$$

where SPI12 is the annual calculated SPI (without dimension), P_i is the annual precipitation for a given year (mm/year), P_{m} is the mean annual precipitation (mm/year) and σ is the temporal standard deviation calculated for each rain gauge during P1 and P2 for annual rainfalls.

Because of its capability to classify the severity of the drought or the humidity, we applied this index in an attempt to assess the spatial and temporal variability over the catchment calculated for the six observed rain gauges during P1 and P2.

Study area and data assessment

Study area

The Raghay catchment is a Mediterranean catchment located in the rural area in the north-western of Tunisia (Fig. 3). This catchment is one of the main tributaries of the high valley of the Medjerda river, which is the only permanent waterway in the country. The length of the main Raghay tributary is about 35 km, which stretches from the confluence with the mainstream network of Medjerda watershed up to the Algerian border and draining an area of 362 km^2 among which almost 40 km^2 being in Algeria (Gara et al. 2015). The catchment has a contrasted topography: having an altitude range varying between 138 and 1183 m, characterized by a high slope in the upstream mountainous part and a weak one in the downstream part, ranging then from 2 to 4%. Dominant land-use types are mostly forest with a typical Mediterranean vegetation cover. The soils are relatively thin, especially in the mountainous part, from 10 to 15 cm at the top of the hill slopes to 120 cm near to the river bed. Soil types are mainly silty loam in the upstream parts and sandy loam in the downstream parts and near the river bed.

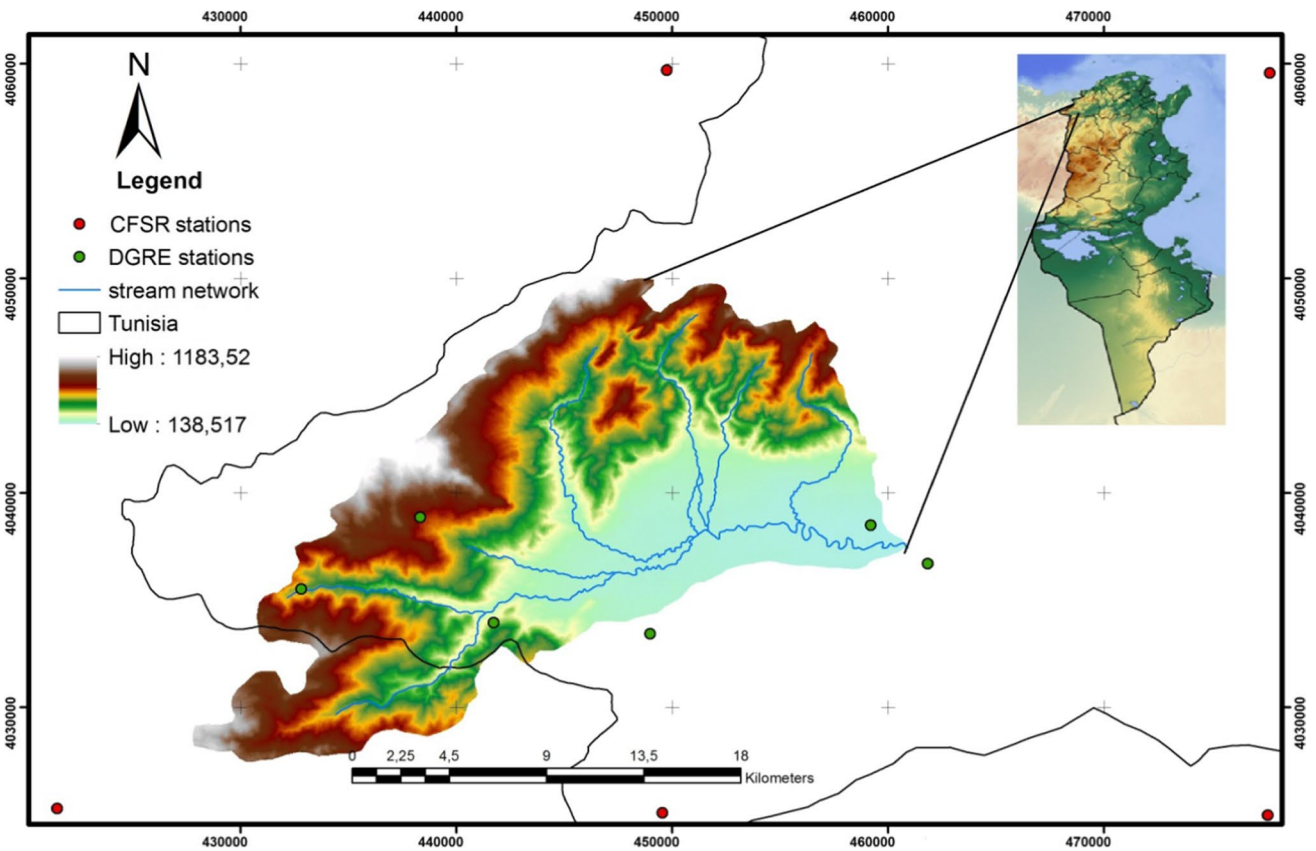

Fig. 3 Location of the Raghay catchment study site

From a climatic point of view, the zone of study presents a certain heterogeneity as it belongs to two different bioclimatic stages: a humid Mediterranean bioclimatic stage with moderate winter and a rainfall from 800 and 1200 mm/year, and a sub-humid bioclimatic stage which receives an annual rainfall varying between 450 and 700 mm/year (Ghorbel 1976). Rainfall is decreasing when going from the Western to the Eastern part in the catchment. The runoff generation process in the western part is expected to be different from the eastern part.

The Raghay catchment has a typical Mediterranean climate, with intense rainfall in the fall and winter seasons. Most of the rainfalls are recorded in winter (40 to 50% of the annual rainfall), while only 3% of the annual rainfall occurs in summer. The wet season starts from October to May, and the dry season starts from June to September. The floods mainly occur during very intense rainy events that may reach more than one hundred mm less than 24 h. In February 2012 for instance, a maximum flow of 1490 m^3/s was recorded at the Ghardimaou hydrometric station, controlling a surface area of 1490 km^2 of the Medjerda basin. Simultaneously, 647 m^3/s of the flows was measured in the Raghay discharge station, causing then catastrophic damages affecting downstream cities. The Raghay catchment is considered as a small sub-catchment in the Medjerda basin which has a huge contribution during floods. The great severity of the floods in this catchment is explained by the short rising times of the flow (less than 1 day), related directly to the concentration time (tc) of the catchment and to the initial soil moisture.

The Raghay catchment is a representative study site on which the modelling procedure will be carried on.

Input data

For the model implementation, several inputs are necessary for combining hydro-climatic time-series data and cartographic data.

Cartographic input data

The topography of the study area is illustrated by the digital elevation model (DEM) provided by the Advanced Spaceborne Thermal Emission and Reflection Radiometer (ASTER). This DEM presents a resolution of 30 m for the mission of the 19 June 2014 with the Universal Transverse Mercator (UTM) coordinate system projection. This model with a fine grid mesh resolution allows outlining the elevation of any point at the Raghay catchment. This DEM was used to define the Raghay catchment and to identify the drainage and the slopes of the studied catchment.

Conventional time-series data

The daily observed rainfall and runoff data of the Raghay catchment were provided by the Tunisian General Directorate of Water Resources (DGRE). The rainfall was measured with six rain gauges (Table 2). These rain gauges have a weak percentage of gaps varying between a minimum gap ratio of 2% at the Raghay Supérieur rain gauge and a maximum gap ratio of almost 11% for the recorded period 1979–2008 at the Feija SM station. The rain gauge stations exhibit a large altimetry variation. The Chemtou Ferme station, for instance, situates at the minimum altitude of 172 m, while the Feija SM station situates at the maximum altitude of 730 m. In order to highlight the spatial variability for the Raghay catchment, we calculated several statistical parameters for the same durations, and then, we compared between the spatially distant rain gauges' values. The large spatial variability is confirmed with descriptive statistical parameters calculated separately for each station, such as the mean annual rainfalls, the standard deviation (σ) and the coefficient of variation (CV), permitting to highlight the importance of using several rain gauges in the Raghay (Table 3). The σ measures the temporal dispersion of the data around the annual mean rainfalls for each rain gauge. For the observed stations, σ varies between 124 mm (Chemtou Ferme station) and 265 mm (Feija SM) proportional to the mean annual rainfall values (417 mm and 967 mm for Chemtou Ferme station and Feija SM, respectively). The CV, which is the percentage of the ratio between σ and the mean annual rainfalls, is greater than 20% affirming the large spatial viability in the Raghay catchment for the conventional rainfall data. This result is consistent with studies emphasizing the large spatiotemporal variability of rainfall in Medjerda catchment (Gader et al. 2015). Based on the results reported for the rainfall observed data, it can be confirmed that the Raghay catchment presents a large spatial and temporal rainfall annual variability.

Runoff data were collected at the hydrometric discharge station 'Raghay Plaine.' The water levels were registered via a mechanical OTT 20™ stream gauge, between 1969 and 2008.

The minimum and maximum temperatures were measured at Jendouba meteorological station and controlled by the National Institute of Meteorology.

The common period of observation for the climatic and hydrometric data for the Raghay catchment is from 1990 to 2008, and it will be adopted for model implementation.

CFSR data

Data from a single observed climatic station for assessing PE is considered insufficient compared to the available spatially distributed observed rainfall data. To increase

Table 2 Detailed description of different hydro-climatic input data used in the SCS-SMA LR model implementation of the Raghay catchment

	Data type	Source	Coordinates UTM[a] (m)			Starting year	Period of observation	Gaps[b] (%)
			X	*Y*	*Z*			
Raghay Plaine	Daily runoff	DGRE[c]	460,817	4,037,710	145	1969	1990–2008	0
Chemtou Raouedet SM	Daily rainfall	DGRE	459,198	4,038,783	179	1966	1967–2012	2
Chemtou Ferme	Daily rainfall	DGRE	461,828	4,036,984	172	1969	1969–2012	4
Feija SM	Daily rainfall	DGRE	438,327	4,039,153	730	1889	1980–2010	11
Oued Mliz	Daily rainfall	DGRE	448,968	4,033,722	200	1973	1974–2012	5
Raghay Supérieur	Daily rainfall	DGRE	441,727	4,034,231	310	1977	1978–2012	2
Sraya Ecole	Daily rainfall	DGRE	432,827	4,035,805	600	1969	1975–2008	6
Jendouba climate station	Daily weather data[d]	INM[e]	449,166	4,033,752	143	1949	1985–2015	1
36481	Daily weather data	CFSR[f]	449,542	4,025,366	1041	1979	1979–2014	0
36484	Daily weather data	CFSR	477,574	4,025,248	860	1979	1979–2014	0
36488	Daily weather data	CFSR	477,664	4,059,878	229	1979	1979–2014	0
36784	Daily weather data	CFSR	421,824	4,060,206	374	1979	1979–2014	0
36788	Daily weather data	CFSR	449,744	4,059,996	306	1979	1979–2014	0

[a]UTM: Universal Transverse Mercator coordinate system, Zone 32 Carthage North

[b]The percentage of the gaps is calculated for the common period of available climatic data: 29 years starting from 1979 to 2008

[c]In situ data obtained for free from the General Directorate of Water Resources, Ministry of Agriculture and Water Resources

[d]Weather described data are: rainfall, maximum temperature, minimum temperature, wind speed, relative humidity, solar radiation

[e]In situ data obtained from National Institute of Meteorology in Tunisia

[f]Reanalysis data obtained from: https://globalweather.tamu.edu/

the spatial resolution of PE input data, global reanalysis data are useful data to represent the spatial distribution patterns of observed weather data (Zhang et al. 2013; Dile and Srinivasan 2014). We used the National Centers for Environmental Prediction's Climate Forecast System Reanalysis (CFSR) climate data to increase the spatial resolution of PE.

The CFSR is a worldwide, high resolution, coupled atmosphere–ocean–land surface-sea ice data system created in order to estimate weather data. The data are provided by the National Centers for Environmental Prediction (NCEP), which produces daily data for precipitation, maximum and minimum temperature, wind speed, relative humidity and solar radiation for the period of 1979–2014 with a resolution of 38 km (Tolera et al. 2018; Saha et al. 2010). All available conventional and satellite observations are included in the CFSR. Satellite observation data are integrated for radiance and are bias-corrected with a full-resolution 'spin-up' runs, taking into account green gas emissions. The CFSR data are completed by a spectral model including the parameterization of all major physical processes (Roth and Lemann 2016). After the calculation of the PE with the method described in "The modified runoff model with PE integration" section, we assessed the same description and statistical parameters as for the rainfall observed data. This allowed validating the use of these reanalysis data and evaluating the distributed or lumped implementation of the RR model (Tables 2, 3). We reveal a large spatial variability of rainfall reanalysis data confirmed by high σ and CV for the mean annual reanalysis rainfall data.

For the PE data, the σ and CV are considered weak since spatial variability for temperature, which is the major driver for PE, is an order of magnitude smaller than for rainfall. For PE, CV is calculated as the percentage of the ratio between σ and the mean annual PE. When having a CV greater than 1%, PE calculated using CFSR data is variable compared to the mean values, validating the use of additional PE data derived from the CFSR data. We further compared between the available observed rainfalls recorded from six rain gauge stations and the rainfalls provided by the gridded CFSR reanalysis data, using ranked box plots and exceedance probability plots. We assessed the comparison in the distribution of the two types of data based on several evaluation criteria for each rank. The rainfall reanalysis data were only used in this paper for comparison with observed rainfalls in order to validate the use of this source of data. As observed rainfall data are spatially distributed, the model was implemented using only these data. In order to obtain spatially distributed PE, the CFSR data were applied for the Raghay catchment, which makes it possible to fill in the gaps in the PE to be integrated into the modelling implementations.

Table 3 Spatial variability description of observed rainfall and mixed PE (gridded data and observed data) of the Raghay catchment

	Rainfall (1979–2008)			Potential evapotranspiration (1990–2008)[a]		
	Mean annual rainfall[b] (mm)	SD[c] (σ)	Coefficient of variation[d]	Mean annual PE[e] (mm)	SD[f] (σ)	Coefficient of variation[g]
Chemtou Raouedet SM	446	124.96	27.99	–	–	–
Chemtou Ferme	417	133.55	31.95	–	–	–
Feija SM	967	265.35	27.42	–	–	–
Oued Mliz	497	142.46	28.63	–	–	–
Raghay Supérieur	508	163.57	32.14	–	–	–
Sraya Ecole	635	188.28	29.63	–	–	–
Jendouba climate station	381	97.81	25.67	1134	25.99	2.29
36481	857	193.99	22.62	1064	26.75	2.51
36484	723	166.95	23.09	1079	23.59	2.18
36488	636	154.97	24.35	1094	23.05	2.1
36784	826	177.26	21.45	1077	20.69	1.91
36788	746	164.86	22.09	1090	20.85	1.91

[a]PE is calculated only for the common period of observation between rainfalls and runoffs

[b]Mean annual rainfalls (mm): the mean annual rainfalls calculated for the observed and CFSR rain gauges during the period of observation 1979–2008

[c]SD (σ) is the temporal standard deviation for annual rainfalls calculated for the observed and CFSR rain gauges during the period of observation 1979–2008

[d]Coefficient of variation (CV) is the temporal coefficient of variation for annual rainfalls calculated for the observed and CFSR rain gauges during the period of observation 1979–2008

[e]Mean annual PE (mm) is the mean annual PE calculated for the climatic stations, during 1990–2008

[f]SD (σ) is the temporal standard deviation for annual PE calculated for the climatic stations, during 1990–2008

[g]Coefficient of variation (CV) is the temporal coefficient of variation for annual PE calculated for the climatic stations, during 1990–2008

Results and discussion

Comparison between observed data (DGRE) and reanalysis gridded data (CFSR)

DGRE and CFSR rainfall for the Raghay catchment were compared on a statistical and graphical basis. Based on ranked box-plot (BP) representation of rainfall for the two types of data (Fig. 4), extreme high rainfall data having an appearance probability (AP) of 5% are similar, with a value of approximately 25 mm/day. However, there is a high difference for mean rainfall values between CFSR data and DGRE data, where CFSR data vary between 1 to 9 mm/day and DGRE data vary between 1 to 4 mm/day, with an AP of 50%. The presence of dry days in the Raghay catchment is validated in both cases of data based on weak and extremely weak AP in the BP having then the highest probability to occur in both cases (respectively, 70 and 95%).

The ranked exceedance probability (EP) was also assessed to give a detailed comparison of the two types of rainfall data (Fig. 5). For the high rainfall values, DGRE data and CFSR have almost the same AP (for EP with 5 and 10% of AP). The difference is clear for rainfall values with a medium AP (50%) in which DGRE data are lower than CFSR data. For dry days, when no rainfalls are recorded, both CFSR and DGRE data had a similar high and extreme high AP (respectively EP for 70% and 95% of AP). Thus, these results are consistent with the results obtained for the BP.

A large similarity was revealed between the extreme values of CFSR and DGRE data, with, respectively, a Nash–Sutcliffe (NS) higher than 85% and a coefficient of determination (R^2) higher than 90%, affirming that the two types of data have similar AP. These results demonstrate the appropriateness of the reanalysis data for flooding studies in Mediterranean poorly gauged catchments.

For EP with AP smaller than 10%, the two types of data are also similar, mainly for data higher than 10 mm/day, confirmed by an NS > 82% and $R^2 > 90\%$. However, the difference is considerable for values smaller than 1 mm/day, confirmed by the AP of 50%. This questions the use of reanalysis data for drought studies in this region.

The estimated differences between the two rainfall types are probably due to the fact that the DGRE rainfall stations

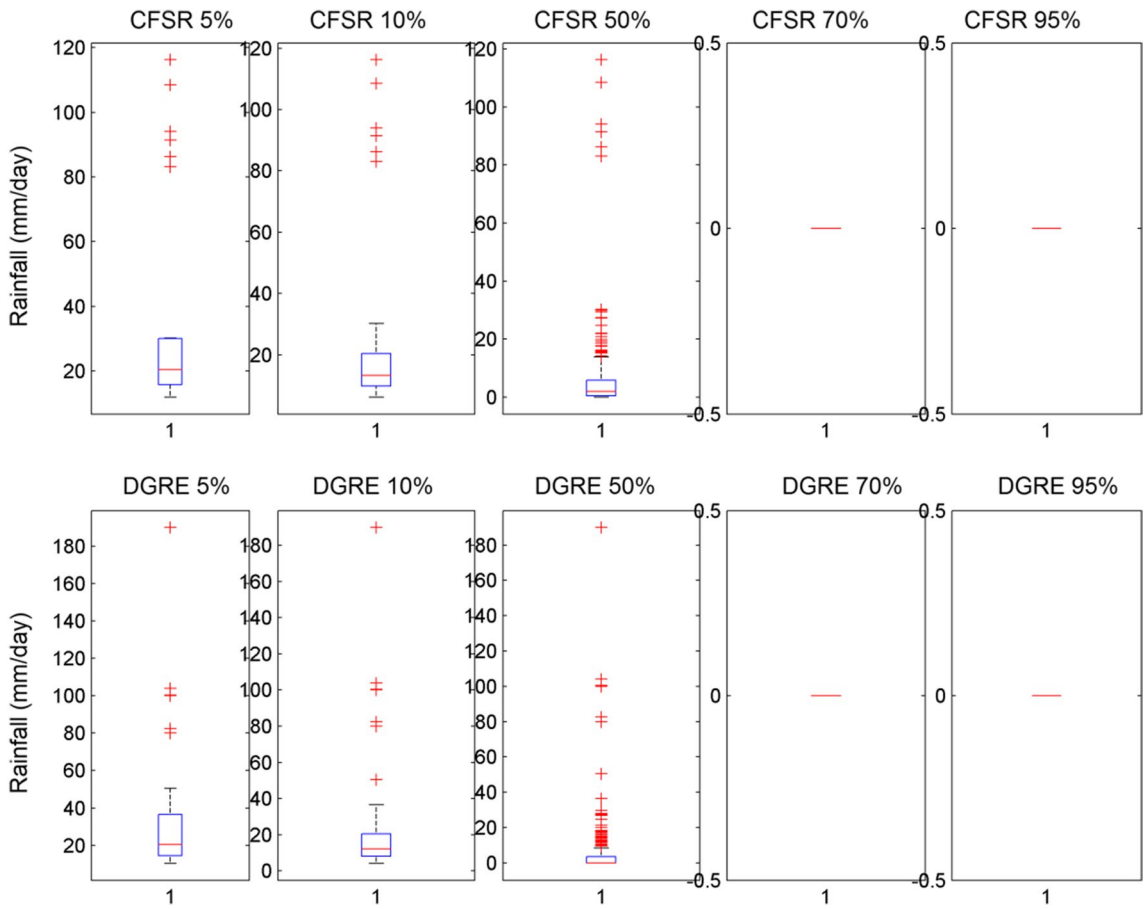

Fig. 4 Ranked box-plot comparison between DGRE data and CFSR data. Five percentage of the recorded data: extremely high recorded rainfall values with a lower probability of appearance (extremely rainy days); 10% of the data: high or important recorded rainfall values (with a probability of appearance 10%); 50% of the data: rainfall with a medium probability off appearance; 70% and 95%: weak and extremely weak rainfall values: they represent dry days with no recorded rainfall having the highest probability of appearance)

are located quite far away from the CFSR grid points (22 to 55 km), which can seriously affect CFSR efficiency in a mountainous area. Generally, reanalysis data overestimate rainfall data with about 20% compared to the observed ones in the study catchment. This difference is essentially caused by weak rainfall having values lesser than 1 mm/day. These results are coherent with the results obtained in other studies. According to Dile and Srinivasan (2014), there is no significant difference between the water balance simulation using conventional weather data and CFSR data, but the average annual rainfall from CFSR weather was higher than the annual rainfall from the conventional weather. Similarly, Fuka et al. (2014) affirmed that adding CFSR data to the suite of watershed modelling tools provides new opportunities for meeting the challenges of modelling in a watershed with scarce climate data.

To run the model, we used the PE derived from the six climatic stations available in the study site with PE calculated from climate data provided by the climatic station of Jendouba in addition to five CFSR climatic reanalysis stations. For the rainfalls, we used the observed data provided from six rain gauges available for the Raghay catchment.

Rainfall–runoff modelling results comparison

The previously described model was implemented in the study area with two types of data schemes: firstly we run the RR model using distributed PE and rainfall, and secondly, using mean areal values of rainfall and PE, interpolated with the Thiessen interpolation method. We evaluated the two types of modelling implementations with a cross-validation split-sample test.

Impact of spatial distribution of PE and rainfall on model parameterization

For implementing the model, the parameters ds2(ds2 = 0) and K_0(K_0 = 0.7) were fixed. This last value was empirically deducted from the calibration of more than thirty catchments located in the south of France and having climate similarity

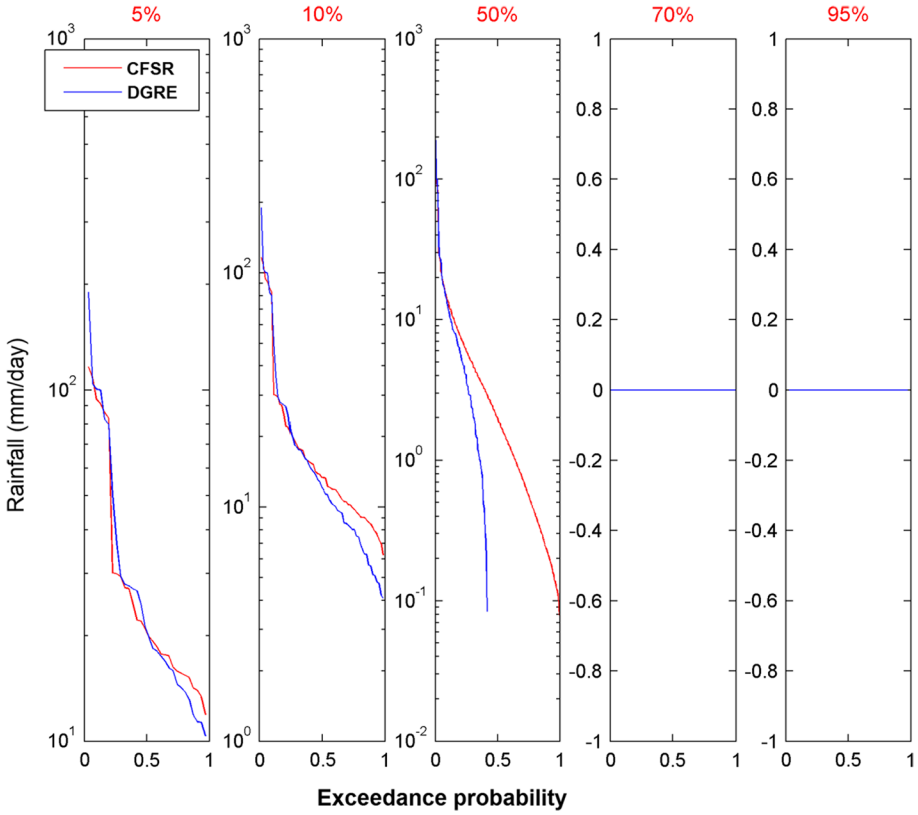

Fig. 5 Ranked exceedance probability comparison between DGRE data and CFSR data. Five percentage of the recorded data: extremely high recorded rainfall values with a lower probability of appearance (extremely rainy days); 10% of the data: high or important recorded rainfall values (with a probability of appearance 10%); 50% of the data: rainfall with a medium probability off appearance; 70% and 95%: weak and extremely weak rainfall values: they represent dry days with no recorded rainfall having the highest probability of appearance)

to the case study. The setting up of these two parameters is intended to make the calibration of the other parameters, such as S, ω, Sa/S and V_0, more robust and in order to minimize the run-time for the RR model.

When we calibrated the RR model for the two phases of the split-sample test, we obtained completely different values for all the parameters for the distributed and lumped modes.

As for the first step of the cross-validation procedure, the value of S for the distributed mode is 122.4 mm. For the lumped case, the S value is around 87.5 mm. The difference is also noticeable for the Sa/S, where we obtain 0.34 and 0.56, respectively, for distributed and lumped modes. The ω parameter reaches 0.82 for the distributed mode and 0.53 for the lumped one.

The value of the S parameter is directly related to the capacity of storage for the soil reservoir which depends on soil characteristics (depth, heterogeneity, porosity, hydraulic conductivity, subsurface dip, etc.). A physical interpretation would be considered to highlight S as the product of the soil depth by the average porosity on a vertical profile (in the case of dominant processes of the contributing area type). This parameter partially explains the runoff rate for each mesh when running the model in the distributed mode. However, for the lumped mode, S was calculated for a unique single mesh. This can explain the differences in the parameter's values between the two types of model implementations.

The Sa/S emphasis the proportion of initial losses in relation to the maximum capacity of the soil reservoir. Generally, the used value of this parameter is fixed to 0.3 (Michel et al. 2005). Nevertheless, we optimized this parameter in order to further highlight the differences in the parameterization for the two model implementations. This optimization featured that the distributed mode yields a parameter value that is approximately similar to the presumed value. It allows concluding that the soil reservoir for the lumped mode lost most of its capacity at the beginning of the calibrated period P1.

The parameter ω reflects the delayed flow that results from the emptying of the upper soil profiles, and it must be calibrated on observed floods. This parameter can be linked to the base flow obtained after the end of the event. According to the values calibrated for this parameter for the two model implementations, it can be presumed that the distributed mode has the biggest fraction of the soil reservoir emptying to contribute to runoff. This leads to a predicted base flow that is higher as compared to the predictions with the lumped mode.

Similar results were obtained for the calibration of the second step of the split-sample test. Yet, the difference is more important, especially for the S parameter varying between 213 mm for the distributed mode and 71 mm for the lumped one. Nevertheless, the difference in the LR model for the two types of model implementations is impossible

to quantify due to the difference in the used parameters. Regarding the lumped mode, the calibrated parameter is K_1 (mn), while for the distributed case it is V_0 (m/s). The differences may be partially related to the model identifiability (Gábor et al. 2017). The BLUE objective function for model optimization relies on the estimated initial parameters before running the model, which may cause errors.

For the distributed mode, there is no significant change in the calibrated V_0 for the two phases of cross-validation with a value of 1.12 m/s for the first step and 0.95 m/s for the second step. Still, the difference is important when calibrating the parameter K_1 for the lumped mode varying between 378 min for the first step of the cross-validation and 1642 min for the second step. This difference highlights variation in the lag, illustrating that the needed time for the produced runoff to reach the outlet for P2 is higher than for P1.

Impact of spatial distribution of PE and rainfall on flow and water amount simulations

The first calibration during the cross-validation process shows that the two model implementations (spatially distributed and lumped) tend to underestimate the peak flow for some flash floods. This underestimation is about 30% compared to the observed peak flow for the two cases and about 19% as a difference in water amount for the distributed mode, while for the lumped one, the difference between predicted and observed water amounts is about 24%. Based on the accuracy parameters comparison, we can highlight a considerable difference between the two model implementations (cases 1 and 2).

For the first case, with a spatially distributed input data, the model gives a NS of 0.61 and a PBIAS of 19.3, which is considered as satisfactory. For the second case, with lumped input data, the modelling is considered unsatisfactory with an NS about 0.57 and a PBIAS of 28.1. The simulated and observed discharges are presented in Fig. 6. The summary of calibrated parameters and accuracy criteria for the two modelling schemes of the first step of the cross-validation test is summarized in Table 4.

For case 1, when using distributed climate input data, the NS is considered acceptable, but the RSR is smaller than 0.7 and the PBIAS is almost unacceptable. Yet, all the accuracy parameters are unacceptable for case 2 when using lumped climatic data. This shows that the goodness of fit for the distributed model is better than for the lumped one. This interpretation is reinforced by the direct comparison between the differences in peak flow and in water amount. This is much higher for the lumped implementation, reaching 45% as for the difference in water amount and 34% for the difference in peak flow. However, for the spatially distributed mode, the difference in water amount and in peak flow is, respectively, 36 and 26%. This observation can be interpreted in terms of

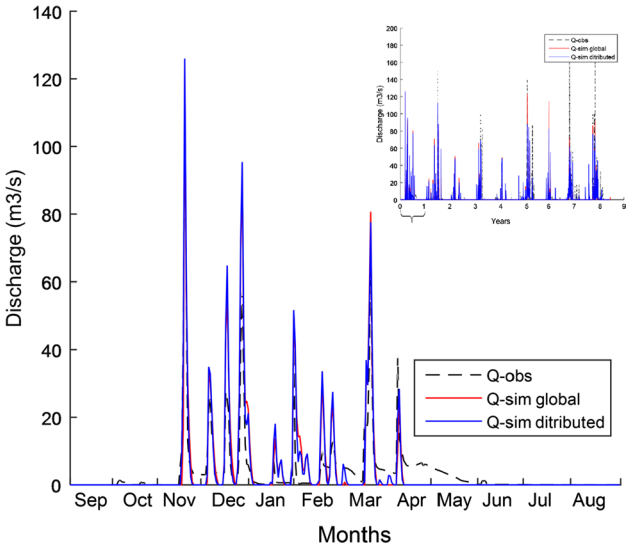

Fig. 6 Comparison between the simulation of the distributed model (case 1) and the global model (case 2) with the observed runoff for the calibration of P1 (first stage of cross-validation calibration): zoom in the first year (September 1990 to August 1991)

the difference between calibrated parameters, especially for the fraction causing the delayed runoff. This difference suggests that the obtained parameters for the distributed mode are more realistic and represent better the hydrological process in the Raghay catchment as compared to the lumped mode.

Another comparison is possible when using a graphical comparison matrix, the scattered plot matrix, comparing at the same time the observed and the simulated runoffs for the two cases. This comparison confirms that the distributed mode significantly yields better results, and it is considered as more efficient to predict runoff at the Raghay catchment for the validation of the first step of cross-validation procedure (Fig. 7).

For the second phase of the split-sample test, we obtained similar results as for the first phase referring to the evaluation criteria (Fig. 8). The distributed mode leads to lesser results than the one found for the calibration of the first step, even if the improvement is much smaller. We found different parameters for the calibration with lumped and distributed data using BLUE optimization. The slightly superior NS results obtained through the distributed mode are associated with a slight improvement of the other accuracy criteria for the calibration procedure as compared with the lumped mode implementation. These results can rely directly on the estimation of initial parameters for calibration, which can significantly improve the modelling optimization for the used objective function.

Our results show therefore that the distributed mode improves the model response for the Raghay catchment,

Table 4 Summary presentation of the calibrated parameters and accuracy criteria for the first step of the split-sample test of the two modelling implementations

	Calibration on P1		Validation on P2	
	Distributed mode (case 1)	Global mode (case 2)	Distributed mode (case 1)	Global mode (case 2)
Calibrated parameters				
S (mm)	122.4	87.5	–	–
ω (dimensionless)	0.82	0.53	–	–
ds2 (1/day)	0	0	–	–
Sa/S (dimensionless)	0.34	0.56	–	–
V_0 (m/s)	1.12	1000	–	–
K_0 (dimensionless)	0.7	0	–	–
K_1 (mn)	0	378.8	–	–
Evaluation criteria				
NS	0.61	0.57	0.55	0.47
RMSE	7.36	7.62	10.43	11.45
RSR	0.48	0.59	0.61	0.74
PBIAS	19.27	28.1	26.7	46.8
EFF	0.15		0.38	

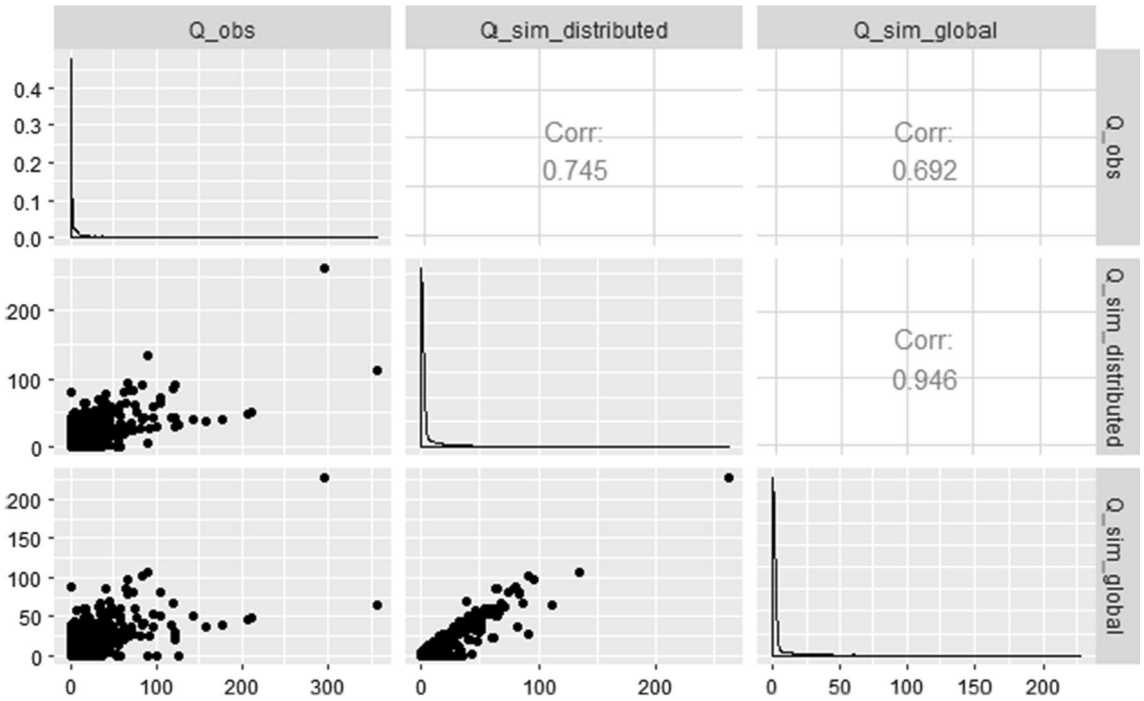

Fig. 7 Scattered plot matrix of the observed versus simulated discharge with global and distributed models in Raghay catchment for the validation of the first part of split-sample test

considering NS, where we obtained superior results for 7% leading to a good NS. Nevertheless, the NS obtained for the lumped mode is only considered as acceptable according to Moriasi et al. (2007). This difference in model responses can be linked to the fact that the model was calibrated and validated for the Raghay catchment for periods P1 and P2 having a completely different hydroclimatic process.

For P1, going from September 1990 to August 1999, the High Valley of Medjerda basin went through a sequence of intense dry periods that marked the drought phenomena in the region (Bargaoui et al. 2008), with only nine important

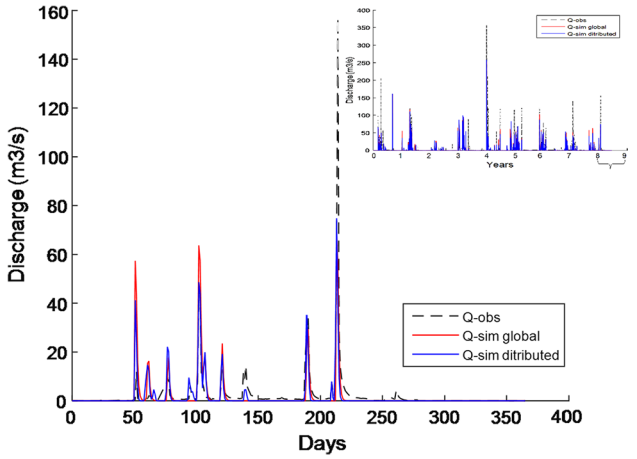

Fig. 8 Comparison between the simulation of the distributed model (case 1) and the global model (case 2) with the observed runoff for the calibration of P2 (second stage of cross-validation calibration): zoom in the last year (September 2007 to August 2008)

events mainly occurred in the autumn season. These events were recorded for the rain gauges located in the mountains and leading to important flash floods in the downstream parts, where no rainfall data were recorded. However, the data for P2 were pronounced with reciprocation of exceptional floods intermitted with intense dry periods. This period was marked by high spatial and temporal variability deducted from the hydro-climatic data, which yielded to note the impact of climate change in the southern Mediterranean region.

A more in-depth assessment is featured when examining the accuracy criteria for the two cases of model implementation (Table 5). For the spatially distributed model, all the accuracy parameters are considered good, with an NS equal to 0.61, an RSR below 0.6 and a PBIAS less than ± 0.15. These evaluation criteria are only considered satisfactory (NS < 0.6, PBIAS $> \pm 0.15$, $0.6 <$ RSR < 0.7) for the lumped model. However, when comparing the differences in peak flow and water amount, the difference is trivial (less than 5%). This result proves that the improvement of the model simulation given by the spatially distributed input is less significant in this phase. This result is more detailed based on the scattered plot matrix, proving that the regression between the two types of simulation is considered as non-significant for this part of the cross-validation procedure (Fig. 9).

By comparing the results obtained for the two phases of split-sample test for the two modelling schemes, we determined the important added value for the distributed model compared with the global one. We demonstrated that using distributed data produces better results for the Raghay catchment, on the basis of several statistical accuracy criteria and graphical comparison. This is consistent with the current state of the art in hydrological modelling. This result ties

Table 5 Summary presentation of the calibrated parameters and accuracy criteria for the second step of the split-sample test of the two modelling implementations

	Calibration on P2		Validation on P1	
	Distributed mode (case 1)	Global mode (case 2)	Distributed mode (case 1)	Global mode (case 2)
Parameters				
S (mm)	213.6	71.7	–	–
ω (dimensionless)	1.31	1.86	–	–
ds2 (1/day)	0	0	–	–
Sa/S (dimensionless)	0.18	0.28	–	–
V_0 (m/s)	0.95	1000	–	–
K_0 (dimensionless)	0.7	0	–	–
K_1 (mn)	0	1642.4	–	–
Evaluation criteria				
NS	0.58	0.55	0.61	0.54
RMSE	9.72	10.19	7.2	7.8
RSR	0.60	0.62	0.59	0.67
PBIAS	24.2	30.4	14.1	19.1
EFF	0.32		0.12	

well but is less pronounced with previous hydrological studies within the Mediterranean catchments using the same platform for hydrological modelling (Tramblay et al. 2011; Coustau et al. 2012). The improvement in our study suggests that ATHYS generally performs better for distributed models than lumped ones. One of the possible explanations for the difference between our study and previous studies with ATHYS in Mediterranean catchments is mainly because the models implemented for these previous cases were event-based with a finer time step and then the daily time step used in this research study. This kind of model implementations directly depends on the initial soil moisture for each event, an issue that does not appear in continuous RR models. Nevertheless, because of the lack of a finer observed data for the studied catchment, we decided to not investigate an infra-daily continuous modelling response.

Another possible explanation is that the hydrological process in Raghay catchment presents a significant fluctuation between dry and wet spells. This fluctuation is clearly noticeable for the part P2 of the data where the effect of climate change was highly prevalent.

As for the time step selected for this case of study, we opted to use the daily hydro-climatic data. To confirm this choice, we calculated the tc through several formulas. We obtained a large difference between the obtained results, between 9 and 22 h, according to the used formula and to

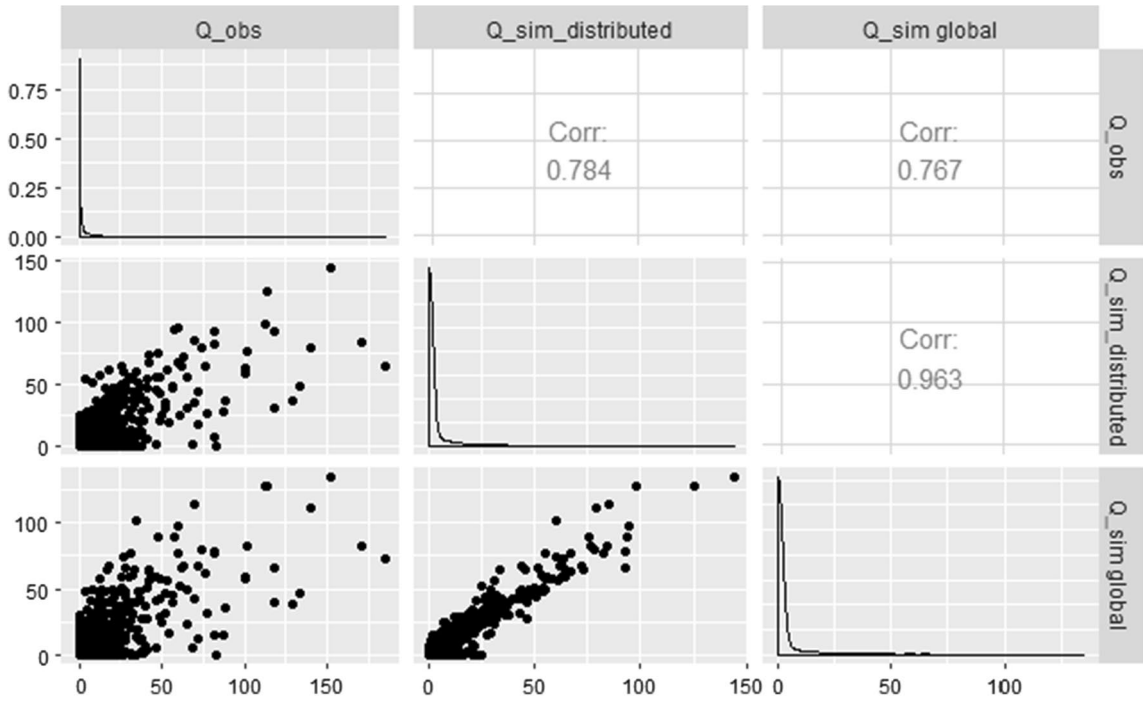

Fig. 9 Scattered plot matrix of the observed versus simulated discharge with global and distributed models in Raghay catchment for the validation of the second part of split-sample test

the estimated curve number. The obtained results are in concordance with the ones obtained by Fang et al. (2008), who used five different formulas to calculate the tc. The obtained values of tc are varying between 13 and 20 h for catchments with similar areas as for our case of study. The time of concentration of the catchment is thus less than 1 day. However, the purpose of this paper was to demonstrate the added value of the spatial distribution of rainfall and potential evapotranspiration (PE) in the prediction of the discharge for a small Mediterranean catchment. The fact that the time of concentration is less than 1 day when using daily rainfall data is not a problem, provided the models when compared with the same time step of the input rainfalls: spatially distributed or averaged rainfalls. Furthermore, the fact that the time of concentration is less than the time step of the input data makes that the model cannot retrieve accurate estimation of the flood dynamics. So it cannot be applied for hydrological applications such as flood forecasting, because the daily discharge could be much less that the instantaneous peak flow. But the model could be convenient for assessing water resources or hydrological budgets, which the daily discharges are convenient for.

We remark that for the two cases of modelling implementations, the RR model underestimates several important floods occurring in the autumn season. For some cases, the lumped mode overestimates the base flow, especially in the validation of the two contrasted phases. However, the running time required by the lumped mode is much less than the time needed for the spatially distributed mode.

When comparing this research study with previous studies using the same time step, many studies claimed that the two model implementations were rather close. Brulebois et al. (2018) pointed out the same conclusion by obtaining rather close results when tested over contrasted climate periods, with minor higher stability for the semi-distributed model. The partial improvement of model efficiency criteria was also assessed by Lobligeois et al. (2014), where they found for a large sample of tested floods and catchment that results were associated with the catchment characteristics. As discussed, the Raghay catchment presents some improvements in terms of accuracy when using spatially distributed rainfall and PE data.

Impact of spatial distribution of PE and rainfall on the flow duration curve (FDC) at the Raghay catchment

Among the various indicators of runoff variability in watersheds, FDC of daily flow was assessed in this part to give a further comparison between distributed and lumped modes. The FDC represents the relationship between the magnitude and frequency of stream flows at the catchment discharge point when an adequate number of stream-flow observations are available (Botter et al. 2008). These observations may have different time step of entries;

however, mean daily stream-flow values are generally used (Ganora et al. 2009). Due to their ability to give a simple and comprehensive graphical view of the overall historical variability of stream flows over the catchment, from floods to low flows, empirical FDCs are widely used to represent the runoff regime in several water-related studies (Pugliese et al. 2014; Castellarin et al. 2004). We can virtually arrange the flow percentiles into three different ranks with different intervals of FDC: high flow for the segment between 0 and 10% of time flow equal or exceeded, median flows (segment between 10 and 50%) and low flows (segment between 50 and 100%).

The 9-year FDC obtained for the validation of the first step of the split-sample test highlights a large difference between the two modelling cases (Fig. 10). For the segment with values below 10%, there is a large resemblance for the two cases compared with the observed FDC, with a slight preference to the distributed mode. However, the difference is quite considerable for the two segments of median flows and low flows, respectively (10–50%) and (50–100%). Overall, the distributed mode gives better predicted FDC than the one predicted for the lumped mode for the first step of cross-validation.

Concerning the 9-year FDC obtained for the validation of the second step of the split-sample test, there is no significant difference between the two modelling cases having almost the same slope (Fig. 11). This is elucidated in "Impact of spatial distribution of PE and rainfall on flow and water amount simulations" section, proving that for the second validation, the difference between the two cases is not significant. Compared to the observed FDC, the difference between the two cases is based on medium and low flows, while the probability of high flows remains the same as for the first validation.

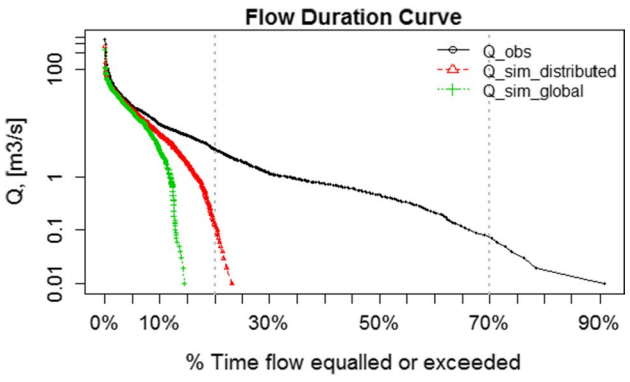

Fig. 10 Nine-year FDC simulation comparison between lumped and distributed modes at the Raghay for the validation of the first step of cross-validation test (validation on P2)

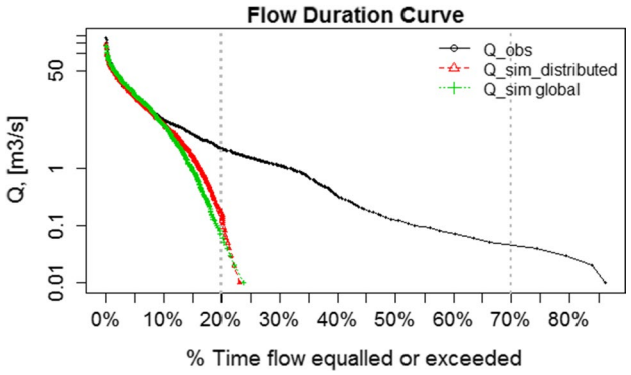

Fig. 11 Nine-year FDC simulation comparison between lumped and distributed modes at the Raghay for the validation of the second step of cross-validation test (validation on P1)

PE and rainfall spatial distribution global impact on flood simulation

In this section, the global impact is assessed based on the EFF, detailed in "Cross-validation procedure and performance evaluation" section. This criterion compares the simulated runoffs of distributed and lumped modes at the same time with the observed ones.

For the first validation, the EFF, about 0.38 which is much greater than 0, proves that the model simulation shows progress using spatially distributed input. However, this difference is less significant for the validation of the second phase of cross-validation, where the EFF is less than the one found in the validation of the first stage (0.12), yet, still higher than 0 confirming then the positive consequence for the use of distributed input data on model efficiency at the Raghay catchment. In order to additionally investigate the origins of the differences between the values of the EFF, we calculated the mean annual values, σ and CV, for annual input values of rainfalls and PE which are introduced to run the model, separately for the two periods of the data, P1 and P2. These mean annual temporal descriptive statistics were calculated for the contrasted durations of 9 years each and for all the spatially distant stations demonstrate a large spatial and temporal variability mainly noticed through the CV. This coefficient presents a noticeable difference during P2 for the rainfalls of the six rain gauges, varying between 17.6 and 34.21%, where during P1, it fluctuates between 23 and 34.7% (Table 6). For the PE, CV is around 2% for the two parts P1 and P2 and for all the climatic stations since the spatial and temporal variability of the mean annual temperature is not really consistent in the studied catchment. However, using spatially distributed data has slightly improved the modelling results. The SPI has been also used as an index to assess the climate variability for the different rain gauges in the Raghay over the contrasted

Table 6 Observed rainfall and mixed PE (gridded data and observed data) used to run the model in the Raghay catchment for the cross-validation periods P1 (1990–1999) and P2 (1999–2008)

	Mean annual (mm)[c]		SD (σ)[d]		Coefficient of variation[e]	
	P1[a]	P2[b]	P1	P2	P1	P2
Rainfall						
Chemtou Raouedet SM	472.99	453.27	145.82	148.55	30.83	32.77
Chemtou Ferme	466.69	452.35	162.09	136.31	34.73	30.13
Feija SM	930.92	844.37	221.74	148.58	23.82	17.60
Oued Mliz	505.04	525.69	160.04	170.94	31.69	32.52
Raghay Supérieur	522.22	557.89	174.92	190.86	33.50	34.21
Sraya Ecole	654.22	540.61	160.25	181.54	24.49	33.58
Potential evapotranspiration						
Jendouba climate station	1135.18	1133.00	30.1	22.95	2.65	2.03
36481	1052.10	1077.78	25.25	22.64	2.40	2.10
36484	1070.01	1088.14	24.76	19.62	2.31	1.80
36488	1085.93	1104.02	24.31	18.84	2.24	1.71
36784	1069.93	1085.15	21.17	18.21	1.98	1.68
36788	1083.23	1097.92	21.63	18.31	2.00	1.67

[a]P1: the part of the data with a duration of 9 years, going from September 1990 to August 1999

[b]P2: the part of the data with a duration of 9 years, going from September 1999 until August 2008

[c]Mean annual (mm): the mean annual rainfalls and PE calculated, respectively, for the observed rain gauges and the climatic stations, during P1 and P2 separately

[d]SD (σ) is the temporal standard deviation for annual rainfalls and PE calculated, respectively, for the observed rain gauges and for the climatic stations, during P1 and P2 separately

[e]Coefficient of variation (CV) is the temporal coefficient of variation for annual rainfalls and PE calculated, respectively, for the observed rain gauges and for the climatic stations, during P1 and P2 separately

periods. During P1, the SPI shows very similar variations for all the rain gauges with only small differences in terms of drought amplitude, varying between severe humidity and severe drought. Nevertheless, during P2, the variability in the SPI calculated between the different rain gauges is really spectacular fluctuating between extreme drought and extreme humidity (Fig. 12). The variability in the SPI during P2 reflects the large variability in the rainfalls. This variability can be explained by different possible origins mainly through the marked climate change impacts in the two last decades where its effects were strengthened by the important difference in altitudes and slopes over the Raghay.

Conclusions

In this paper, we assessed the performance of the SCS–SMA LR model with the PE integration, from ATHYS platform. We implemented the conceptual daily continuous model in the Raghay catchment with two different types of implementations: once in a fully spatially distributed mode (case 1) by using spatially distributed rainfall and PE, and once in a lumped mode using Thiessen-interpolated PE and rainfall (case 2). The used model requires a few numbers of parameters to be calibrated letting for simple and efficient modelling phases.

In order to reinforce and to fill in the gaps for the PE data required to run the model in the spatially distributed mode for the studied catchment, we integrated CFSR data in addition to the observed PE provided from one observed climatic station, and the observed rainfalls recorded on the level of six rain gauges.

A cross-validation procedure was implemented on the two equal parts of the hydro-climatic data (P1 and P2) for the two modelling cases. The main conclusions that can be drawn for the validation of the first and second phases of the split-sample test is that the RR model presents a slight preference to the spatially distributed implementations, on the basis of different model accuracy criteria (NS, RSR, RMSE, PBIAS and EFF) which are performing less good in the lumped mode. However, this improvement is not important, especially for the NS accuracy criterion, which is presenting a difference that does not exceed 7%, for the calibration and for the validation of the part P2 of the data.

To further investigate the two modelling cases response, we integrated graphical and statistical comparisons, such as the scattered plot matrix showing the difference between observed and simulated runoffs for the two cases, and the 9-year duration FDCs for the two cases of model

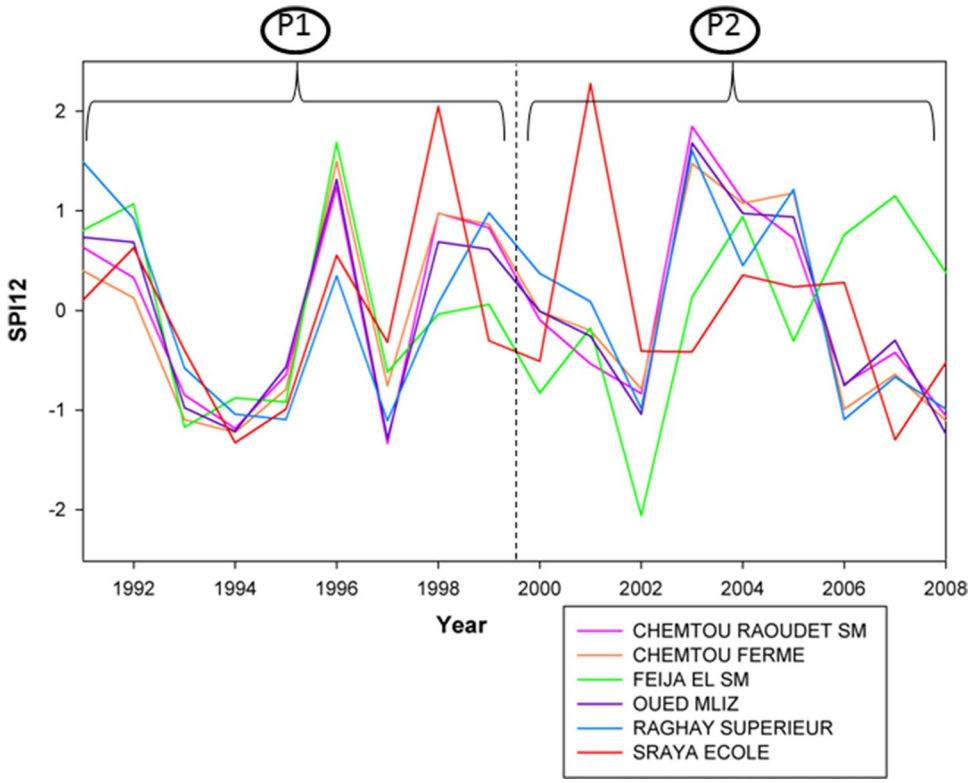

Fig. 12 Comparison between the SPI 12 index calculated for the six rain gauges during P1 and P2 in the Raghay catchment

implementations, which were leading to prove the same results found on the basis of the goodness-of-fit criteria.

These findings confirm that according to the validation of the second step of the cross-validation procedure, the improvement of the model simulation given by the spatially distributed input is less significant in this phase, with an EFF = 0.12 as compared to EFF = 0.38 for the validation of the first stage. Nevertheless, these criteria cast the need to use of spatially distributed data because it is higher than 0. Statistical descriptive indexes were calculated for the input data over the contrasted periods, P1 and P2, in an attempt to explain by climate reasoning the obtained difference in the EFF through the cross-validation procedure. These statistical coefficients reinforced the large spatial and temporal variability in the rainfalls for the second part of the data, P2. The SPI also confirmed this assumption when giving a large variability in its values for the different rain gauges as for the same period, P2.

Based on the analyses and the results reported in this study, it can be concluded that spatially distributed rainfall and PE increase the efficiency of the model in the Raghay catchment. However, this improvement is less important for the second half part of the data, P2, used in this comparison study. The interest of the spatial distribution of rainfalls and PE depends on the spatial and temporal variability of climate data over the catchment. This spatial and temporal variability is mainly controlled by the large variability in the altitudes and the slopes over the catchment coupled with the present impact of climate change assessed in recent decades.

Future research should consider the potential effects of other types of models presented in the ATHYS platform more carefully. For example, the main issue when trying to compare accuracy between models having a different number of input parameters (i.e. conceptual based versus physically based model implementations in the ATHYS platform), we have to refer to other accuracy criteria linking between the number of model parameters and the goodness of fit, in order to evaluate the model efficiency. The goodness-of-fit criteria give only a partial understanding of model performance that should be completed with an additional parsimony analysis. This is an issue for future research to explore.

It could be also with great importance to apply the same methodology for other catchments situated in the Medjerda basin in Tunisia. However, the availability of distributed climate data needed to calculate PE remains the main challenge for Tunisian catchments. Further simplifications may be possible by using a unique PE for each catchment, based on the assumption that the NS rarely exceeds 1% when using spatially distributed PE.

We believed that apart from looking for model responses in the actual conditions, it would be an objective for future studies to investigate how different these two models will produce the projected hydrological process for the studied catchment under different climate change scenarios' projections. This will aim to replicate the differences in the results

of the two model schemes regardless of their complexity. Future investigations are necessary to summarize this kind of comparisons.

Acknowledgements This research was realized at the Sustainable Management of Water and Soil Resources (UR17AGR03). The authors received funding from the project 'Adaptation of water resources management in the Medjerda watershed to the challenges of climate change' through the project 11—axis 2 of the Wallonia Brussels International Grant No. (Aso/CFo/Tunisie/15.1218/cf) and Tunisia Joint Commission 2016–2018. Moreover, part of this research study was accomplished in the Laboratory of HydroSciences in Montpellier with the funding of mobility program provided by the Ministry of Higher Education and Scientific Research in Tunisia. Authors also would like to thank the Tunisian General Directorate of Water Resources (DGRE) for providing conventional data for the study area. Finally, the authors would like to express their gratitude for the anonymous reviewers of this paper.

Compliance with ethical standards

Conflict of interest On behalf of all authors, the corresponding author states that there is no conflict of interest.

References

Ajami NK, Gupta H, Wagener T, Sorooshian S (2004) Calibration of a semi-distributed hydrologic model for streamflow estimation along a river system. J Hydrol 298:112–135. https://doi.org/10.1016/J.JHYDROL.2004.03.033

Andréassian V, Oddos A, Michel C, Anctil F, Perrin C, Loumagne C (2004) Impact of spatial aggregation of inputs and parameters on the efficiency of rainfall–runoff models: a theoretical study using chimera watersheds. Water Resour Res. https://doi.org/10.1029/2003WR002854

Apip Sayama T, Tachikawa Y, Takara K (2012) Spatial lumping of a distributed rainfall–sediment–runoff model and its effective lumping scale. Hydrol Process 26:855–871. https://doi.org/10.1002/hyp.8300

Bao H, Wang L, Zhang K, Li Z, Wang L (2017) Application of a developed distributed hydrological model based on the mixed runoff generation model and 2D kinematic wave flow routing model for better flood forecasting. Atmos Sci Lett 18:284–293. https://doi.org/10.1002/asl.754

Bargaoui Z, Hamouda D, Houcine A (2008) Modélisation pluie-débit et classification hydroclimatique. Rev des Sci l'eau 21:233–245. https://doi.org/10.7202/018468ar

Bentura PLF, Michel C (1997) Flood routing in a wide channel with a quadratic lag-and-route method. Hydrol Sci J 42(2):169–189

Botter G, Zanardo S, Porporato A, Rodriguez-Iturbe I, Rinaldo A (2008) Ecohydrological model of flow duration curves and annual minima. Water Resour Res. https://doi.org/10.1029/2008WR006814

Bouvier C, Marchandise A, Brunet P, Crespy A (2008) Un modèle pluie-débit distribué événementiel parcimonieux pour la prédétermination et la prévision des crues éclair en zone méditerranéenne. Application au bassin du Gardon d'Anduze. IWRA congress 2008, p 10. https://www.iwra.org/congress/2008/resource/authors/abs811_article.pdf. Accessed 23 June 2018

Bouvier C, Crespy A, L'Aour-Dufour A, Crès FN, Desclaux F, Marchandise A (2013) Distributed hydrological modeling—the ATHYS platform. Modeling software. Wiley, Hoboken, pp 83–100

Breuer L, Huisman JA, Willems P, Bormann H, Bronstert A, Croke B, Frede H, Gräff T, Hubrechts L, Jakeman A, Kite G, Lanini J, Leavesley G, Lettenmaier D, Lindström G, Seibert J, Sivapalan M, Viney N (2009) Assessing the impact of land use change on hydrology by ensemble modeling (LUCHEM). I: model intercomparison with current land use. Adv Water Resour 32:129–146. https://doi.org/10.1016/j.advwatres.2008.10.003

Brocca L, Melone F, Moramarco T, Wagner W, Naeimi V, Bartalis Z, Hasenauer S (2010) Improving runoff prediction through the assimilation of the ASCAT soil moisture product. Earth Syst Sci 145194:1881–1893. https://doi.org/10.5194/hess-14-1881-2010

Brulebois E, Ubertosi M, Castel T, Richard Y, Sauvage S, Sanchez Perez JM, Le Moine N, Amiotte-Suchet P (2018) Robustness and performance of semi-distributed (SWAT) and global (GR4J) hydrological models throughout an observed climatic shift over contrasted French watersheds. Open Water J 5(1):41–56. https://scholarsarchive.byu.edu/openwater/vol5/iss1/4

Castellarin A, Galeati G, Brandimarte L, Montanari A, Brath A (2004) Regional flow-duration curves: reliability for ungauged basins. Adv Water Resour. https://doi.org/10.1016/j.advwatres.2004.08.005

Coustau M, Bouvier C, Borrell-Estupina V, Jourde H (2012) Flood modelling with a distributed event-based parsimonious rainfall–runoff model: case of the karstic Lez river catchment. Nat Hazards Earth Syst Sci 12:1119–1133. https://doi.org/10.5194/nhess-12-1119-2012

Dakhlaoui H, Ruelland D, Tramblay Y, Bargaoui Z (2017) Evaluating the robustness of conceptual rainfall–runoff models under climate variability in northern Tunisia. J Hydrol 550:201–217. https://doi.org/10.1016/J.JHYDROL.2017.04.032

Dile YT, Srinivasan R (2014) Evaluation of CFSR climate data for hydrologic prediction in data-scarce watersheds: an application in the blue nile river basin. J Am Water Resour Assoc 50:1226–1241. https://doi.org/10.1111/jawr.12182

Duan Q, Gupta HV, Sorooshian S, Rousseau A, Turcotte R (2003) Calibration of watershed models. American Geophysical Union, Washington

Fang X, Thompson DB, Cleveland TG et al (2008) Time of concentration estimated using watershed parameters determined by automated and manual methods. J Irrig Drain Eng 134:202–211. https://doi.org/10.1061/(ASCE)0733-9437(2008)134:2(202)

Fuka DR, Walter MT, Macalister C, Degaetano A, Steenhuis T, Easton Z (2014) Using the climate forecast system reanalysis as weather input data for watershed models. Hydrol Process. https://doi.org/10.1002/hyp.10073

Gábor A, Villaverde AF, Banga JR (2017) Parameter identifiability analysis and visualization in large-scale kinetic models of biosystems. BMC Syst Biol 11:54. https://doi.org/10.1186/s12918-017-0428-y

Gader K, Gara A, Slimani M, Mahjoub MR (2015) Study of spatio-temporal variability of the maximum daily rainfall. In: 2015 6th International conference on modeling, simulation, and applied optimization (ICMSAO). IEEE, pp 1–6

Ganora D, Claps P, Laio F, Viglione A (2009) An approach to estimate nonparametric flow duration curves in ungauged basins. Water Resour Res. https://doi.org/10.1029/2008WR007472

Gara A, Gader K, Bergaoui M, Mahjoub MR (2015) Assessment of the hydrological response of the watershed through a distributed physically-based modeling for extreme events: application in the Raghay catchment (Medjerda) (Northern Tunisia). In: 6th international conference on modeling, simulation, and applied optimization, ICMSAO 2015. IEEE, pp 1–6

Ghorbel A (1976) Etude hydrologique de l'oued Rarai. 26

Hawkins RH (1993) Asymptotic determination of runoff curve numbers from data. J Irrig Drain Eng 119:334–345. https://doi.org/10.1061/(ASCE)0733-9437(1993)119:2(334)

Henderson CR (1975) Best linear unbiased estimation and prediction under a selection model. Biometrics 31:423. https://doi.org/10.2307/2529430

Ibrahim B, Wisser D, Barry B, Fowe T, Aduna A (2015) Hydrological predictions for small ungauged watersheds in the Sudanian zone of the Volta basin in West Africa. J Hydrol Reg Stud 4:386–397. https://doi.org/10.1016/J.EJRH.2015.07.007

Khakbaz B, Imam B, Hsu K, Sorooshian S (2012) From lumped to distributed via semi-distributed: calibration strategies for semi-distributed hydrologic models. J Hydrol 418–419:61–77. https://doi.org/10.1016/J.JHYDROL.2009.02.021

Klemeš V (1986) Operational testing of hydrological simulation models. Hydrol Sci J. https://doi.org/10.1080/02626668609491024

Koren V, Zhang Z, Zhang Y, Reed SM, Cui Z, Moreda F, Cosgrove BA, Mizukami N, Anderson EA (2012) Results of the DMIP 2 Oklahoma experiments. J Hydrol 418–419:17–48. https://doi.org/10.1016/J.JHYDROL.2011.08.056

Lewis D, Singer MJ, Tate KW (2000) Applicability of SCS curve number method for a California oak woodlands watershed. J Soil Water Conserv 55:226–230

Liu X, Li J (2008) Application of SCS model in estimation of runoff from small watershed in Loess Plateau of China. Chin Geogr Sci 18:235. https://doi.org/10.1007/s11769-008-0235-x

Lobligeois F, Andréassian V, Perrin C, Tabary P, Loumagne C (2014) When does higher spatial resolution rainfall information improve streamflow simulation? An evaluation using 3620 flood events. Hydrol Earth Syst Sci 18:575–594. https://doi.org/10.5194/hess-18-575-2014

Ludwig R, Roson R, Zografos C, Kallis G (2011) Towards an interdisciplinary research agenda on climate change, water and security in Southern Europe and neighboring countries. Environ Sci Policy. https://doi.org/10.1016/j.envsci.2011.04.003

Mckee TB, Doesken NJ, Kleist J (1993) The relationship of drought frequency and duration to time scales. In: Eighth conference on applied climatology, pp 179–184

Michel C, Andréassian V, Perrin C (2005) Soil conservation service curve number method: How to mend a wrong soil moisture accounting procedure? Water Resour Res. https://doi.org/10.1029/2004wr003191

Mishra SK, Singh VP, Sansalone JJ, Aravamuthan V (2003) A Modified SCS-CN Method: characterization and Testing. Water Resour Manag 17:37–68. https://doi.org/10.1023/A:1023099005944

Moriasi DN, Arnold JG, Van Liew MW, Bingner R, Harmel R, Veith T (2007) Model evaluation guidelines for systematic quantification of accuracy in watershed simulations. Trans ASABE 50:885–900

Nash JE, Sutcliffe JV (1970) River flow forecasting through conceptual models part I—a discussion of principles. J Hydrol 10:282–290. https://doi.org/10.1016/0022-1694(70)90255-6

Oudin L, Hervieu F, Michel C, Perrin C, Andréassian V, Anctil F, Loumagne C (2005) Which potential evapotranspiration input for a lumped rainfall–runoff model? Part 2—towards a simple and efficient potential evapotranspiration model for rainfall–runoff modelling. J Hydrol 303:290–306. https://doi.org/10.1016/J.JHYDROL.2004.08.026

Oudin L, Andréassian V, Perrin C, Michel C, Le Moine N (2008) Spatial proximity, physical similarity, regression and ungaged catchments: a comparison of regionalization approaches based on 913 French catchments. Water Resour Res. https://doi.org/10.1029/2007WR006240

Pugliese A, Castellarin A, Brath A (2014) Geostatistical prediction of flow-duration curves in an index-flow framework. Hydrol Earth Syst Sci 18:3801–3816. https://doi.org/10.5194/hess-18-3801-2014

Roth V, Lemann T (2016) Comparing CFSR and conventional weather data for discharge and soil loss modelling with SWAT in small catchments in the Ethiopian Highlands. Hydrol Earth Syst Sci 20:921–934. https://doi.org/10.5194/hess-20-921-2016

Saha S, Moorthi S, Pan HL, Wu X, Wang J, Nadiga S, Tripp P, Kistler R, Woollen J, Behringer D, Liu H, Stokes D, Grumbine R, Gayno G, Wang J, Hou Y, Chuang H, Juang H, Sela J, Iredell M, Treadon R, Kleist D, Van Delst P, Keyser D, Derber J, Ek M, Meng J, Wei H, Yang R, Lord S, van den Dool H, Kumar A, Wang W, Long C, Chelliah M, Xue Y, Huang B, Schemm J, Ebisuzaki W, Lin R, Xie P, Chen M, Zhou S, Higgins W, Zou C, Liu Q, Chen Y, Han Y, Cucurull L, Reynolds R, Rutledge G, Goldberg M (2010) The NCEP climate forecast system reanalysis. Bull Am Meteorol Soc 91:1015–1058. https://doi.org/10.1175/2010BAMS3001.1

Sangati M, Borga M (2009) Influence of rainfall spatial resolution on flash flood modelling. Nat Hazards Earth Syst Sci 9:575–584

Schuol J, Abbaspour KC, Yang H, Srinivasan R, Zehnder A (2008) Modeling blue and green water availability in Africa. Water Resour Res. https://doi.org/10.1029/2007WR006609

Sellami H, La Jeunesse I, Benabdallah S, Vanclooster M (2013) Parameter and rating curve uncertainty propagation analysis of the SWAT model for two small Mediterranean catchments. Hydrol Sci J. https://doi.org/10.1080/02626667.2013.837222

Sherman J, Morrison WJ (1950) Adjustment of an inverse matrix corresponding to a change in one element of a given matrix. Ann Math Stat 21:124–127

Singh J, Knapp HV, Demissie M (2005) Hydrologic modeling of the Iroquois river watershed using HSPF and SWAT. J Am Water Resour Assoc 41(2):343–360. https://doi.org/10.1111/j.1752-1688.2005.tb03740.x

Tegegne G, Park DK, Kim Y-O (2017) Comparison of hydrological models for the assessment of water resources in a data-scarce region, the Upper Blue Nile River Basin. J Hydrol Reg Stud 14:49–66. https://doi.org/10.1016/J.EJRH.2017.10.002

Tolera M, Chung I-M, Chang S (2018) Evaluation of the climate forecast system reanalysis weather data for watershed modeling in Upper Awash Basin. Ethiopia. Water 10:725. https://doi.org/10.3390/w10060725

Tramblay Y, Bouvier C, Ayral P-A, Marchandise A (2011) Impact of rainfall spatial distribution on rainfall–runoff modelling efficiency and initial soil moisture conditions estimation. Nat Hazards Earth Syst Sci 11:157–170. https://doi.org/10.5194/nhess-11-157-2011

Vansteenkiste T, Tavakoli M, Van Steenbergen N, De Smedt F, Batelaan O, Pereira F, Willems P (2014) Intercomparison of five lumped and distributed models for catchment runoff and extreme flow simulation. J Hydrol 511:335–349. https://doi.org/10.1016/J.JHYDROL.2014.01.050

Wöhling T, Samaniego L, Kumar R (2013) Evaluating multiple performance criteria to calibrate the distributed hydrological model of the upper Neckar catchment. Environ Earth Sci 69:453–468. https://doi.org/10.1007/s12665-013-2306-2

Zhang Q, Heiner K, Holmgren K (2013) How well do reanalyses represent the southern African precipitation? Clim Dyn. https://doi.org/10.1007/s00382-012-1423-z

Zkhiri W, Tramblay Y, Hanich L et al (2019) Spatiotemporal characterization of current and future droughts in the High Atlas basins (Morocco). Theor Appl Climatol 135:593–605. https://doi.org/10.1007/s00704-018-2388-6